CORROSION SCIENCE AND TECHNOLOGY, Vol.18, No.5(2019), pp.206~211
[Research Paper]
pISSN: 1598-6462 / eISSN: 2288-6524
DOI: https://doi.org/10.14773/cst.2019.18.5.206

Superhard SiC Thin Films with a Microstructure of Nanocolumnar Crystalline Grains and an Amorphous Intergranular Phase

Kwan-Won Lim[1,2], Yong-Sub Sim[1,2], Joo-Youl Huh[1], Jong-Keuk Park[2], Wook-Seong Lee[2], and Young-Joon Baik[2,†]

[1]*Department of Materials Science and Engineering, Korea University, 145 Anam-ro, Seongbuk-gu, Seoul 02842, Republic of Korea*
[2]*Center for Electronic Materials, Korea institute of Science and Technology, 5 Hwarang-ro 14-gil, Seongbuk-gu, Seoul 02792, Republic of Korea*

(Received June 26, 2019; Revised October 04, 2019; Accepted October 24, 2019)

Silicon carbide (SiC) thin films become superhard when they have microstructures of nanocolumnar crystalline grains (NCCG) with an intergranular amorphous SiC matrix. We investigated the role of ion bombardment and deposition temperature in forming the NCCG in SiC thin films. A direct-current (DC) unbalanced magnetron sputtering method was used with pure Ar as sputtering gas to deposit the SiC thin films at fixed target power of 200 W and chamber pressure of 0.4 Pa. The Ar ion bombardment of the deposited films was conducted by applying a negative DC bias voltage 0-100 V to the substrate during deposition. The deposition temperature was varied between room temperature and 450°C. Above a critical bias voltage of -80 V, the NCCG formed, whereas, below it, the SiC films were amorphous. Additionally, a minimum thermal energy (corresponding to a deposition temperature of 450°C in this study) was required for the NCCG formation. Transmission electron microscopy, Raman spectroscopy, and glancing angle X-ray diffraction analysis (GAXRD) were conducted to probe the samples' structural characteristics. Of those methods, Raman spectroscopy was a particularly efficient non-destructive tool to analyze the formation of the SiC NCCG in the film, whereas GAXRD was insufficiently sensitive.

Keywords: *Silicon carbide, Nanocomposite structure, Hardness, Nanocolumnar crystalline grain, Amorphous matrix phase*

1. Introduction

SiC thin films have drawn much attention for their promising mechanical applications such as MEMS [1-3] and X-ray masks [4,5]. This is because of their excellent anti-wear properties, oxidation resistance and chemical inertness. Considering the electronic properties of SiC, the application areas become still wider [6-9]. The hardness is a very important property, especially in mechanical applications. The hardness of conventional bulk SiC materials such as single or polycrystalline SiC materials is approximately 28 GPa [10]. On the other hand, some SiC thin films have been reported to have a hardness greater than 40 GPa, referred to as superhardness, far surpassing the above mentioned bulk hardness [11-16]. Recently, our group reported that SiC thin films exhibiting superhardness have a composite phase microstructure of SiC nanocolumnar crystalline grains (NCCG) of several nanometers in width that are separated by an intergranular amorphous SiC matrix [17,18]. Although the two phases are of the same SiC material, it takes the appearance of a composite microstructure consisting of crystalline fibers aligned in an amorphous matrix. We proposed that it was this microstructure that made the films superhard, as dislocation generation is difficult in nano-size crystal grains and dislocation movement across the amorphous matrix is difficult. Such an interpretation is consistent with the models suggested by Veprek *et al*. [19-21] and Musil [22,23] of nanocomposite thin films consisting of different materials.

Since the crystalline SiC phase is more stable thermodynamically than the amorphous SiC phase, the formation of the amorphous thin film instead of a crystalline film is for kinetic reasons. Musumeci *et al*. [24] studied the effect of the annealing on the crystallization of an amorphous SiC thin film and reported that the crystallization begins to occur above 800 °C. However, Ar ion bombardment during the SiC film deposition can reduce the crystallization temperature to a lower value. In this report, we investigated the role of the major deposition variables

†Corresponding author: yjbaik@kist.re.kr

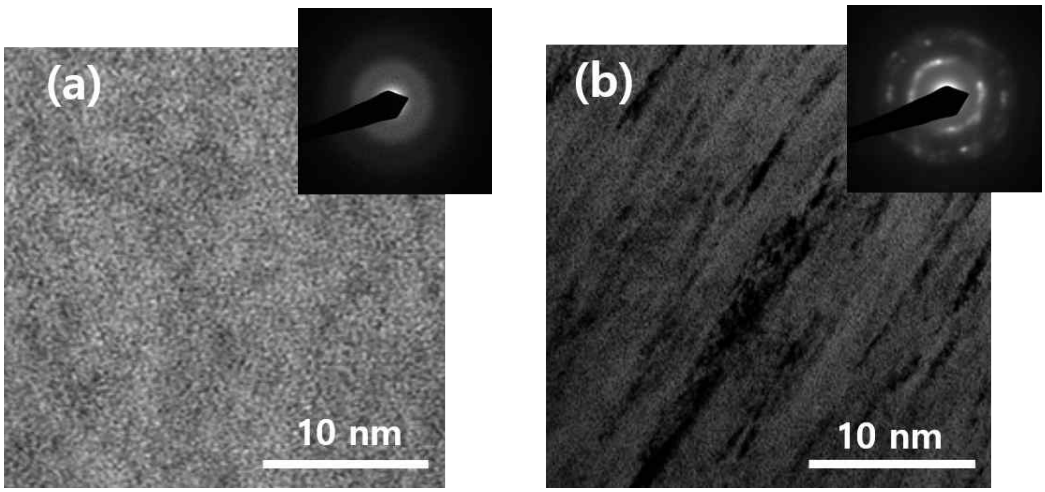

Fig. 1 Cross-sectional TEM images of a SiC film deposited at a bias voltage of (a) 0 V and (b) -80 V.

in forming such a composite-like microstructure. We have chosen the deposition temperature and substrate bias voltage as key deposition variables, as these variables strongly influence the deposited particle energy, which is critical to the determination of the microstructure of the film [25].

2. Experimental Methods

SiC films were grown using an in-house built unbalanced magnetron (UBM) sputtering system (2" diameter UBM sputter gun made by AJA Co., USA) with a sintered silicon carbide target (99.5% purity) connected to a direct current (DC) 200 W electric power source (PSTEK, Inc., model PSPP-0108V3, Korea). High-purity Ar (99.9999%) was used as the sputtering gas, and the distance between the target and substrate was 7.5 cm. We used a (100) plane oriented Si single-crystal wafer as a substrate. The deposition temperature was varied from room temperature to 450 °C, and a DC bias voltage (TRUMPF, Inc., model PBP-2, Germany) between 0 and –100 V was applied to the substrate.

The process chamber was evacuated to a base pressure below 1.6×10^{-4} Pa, and Ar was introduced into the vacuum chamber using a mass flow controller to establish the desired working pressure of 0.4 Pa. The Ar gas flow rate was fixed at 25 cm^3/min. The target was subjected to an Ar pre-sputtering process for 10 min to eliminate the native oxide layer and to stabilize the negative voltage developed at the target. The Si substrates were sputter-cleaned for 15 min with an applied substrate bias of –300 V at 0.4 Pa. Before the sputter-cleaning, the substrates were cleaned in methyl alcohol and acetone for 15 min with sonication to remove organic contaminants. After the sputter-cleaning, the films were deposited at the same pressure for 2 h. Their thicknesses were measured to be approximately 2.4 μm irrespective of the deposition condition.

Cross-sectional images of the films were obtained using both scanning electron microscopy (SEM) (Hitachi, S-4200, Japan) for the thickness measurement, and transmission electron microscopy (TEM) (Tecnai F20 G2). Raman spectroscopy (532 nm Nd:YAG laser, Renishaw, In Via Raman Microscope, UK) was also used for the characterization of the structure of the films with a laser power of 22.5 mW. Glancing angle X-ray diffraction patterns (GAXRD) using a diffractometer were also obtained at a small angle of incidence of 2° using CuKα radiation (Rigaku, D/MAX-2500/PC, Japan) to analyze the lattice structure. The composition of the film was determined via Auger electron spectroscopy (AES) (ULVAC-PHI, Inc., model PHI 710, Japan), and nanoindentation experiments were performed using a Fischerscope HM2000XYp instrument equipped with a Vickers indenter at an indentation load of 10 mN.

3. Results and Discussion

The cross-sectional TEM images of the films enable their classification into two distinct groups of microstructures, depending on the deposition variables. Fig. 1a and 1b show bright-field cross-sectional images of an amorphous SiC film and a SiC film with NCCG, respectively, and the insets show their electron diffraction patterns. The diffraction pattern shown in the inset of Fig. 1a shows a broad diffuse ring pattern, typically found in amorphous structures. Fig. 1b shows the NCCG with col-

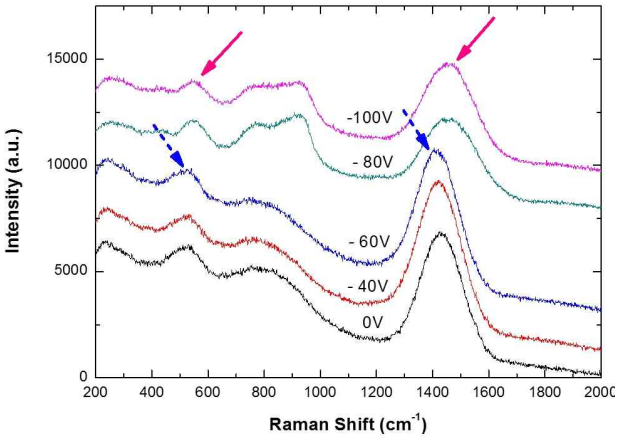

Fig. 2 Raman spectra of SiC films deposited at 450 °C at various substrate bias voltages.

umn widths of several nanometers surrounded by an amorphous matrix, which was presented in detail in our previous report [17]. The diffraction pattern of the latter consisted of broad rings assigned to the amorphous matrix and bright spots originating from the crystalline grains. The amorphous structure was observed for SiC films deposited at low temperatures and small bias voltages, whereas the NCCG structure was observed for films deposited at high temperatures with high bias voltages. Such a microstructural difference resulted in a large difference in the measured hardness: approximately 30 GPa for the amorphous films and approximately 45 GPa for the NCCG-containing films.

The Raman spectra contain the most interesting information on the short-range ordering of the silicon carbide thin films. Fig. 2 shows the Raman spectra of the SiC films deposited at 450 °C at various bias voltages. The spectra show three different bands, which are typically observed for SiC thin films [15,26]: the band at approximately 480-560 cm^{-1} corresponds to silicon clusters, associated with Si–Si bonds; the band at approximately 820 cm^{-1} is associated with Si–C bonds [27]; and the band at approximately 1440 cm^{-1} corresponds to carbon clusters, associated with C–C bonds (the intensity of the C–C band appears large relative to the actual volume fraction of the Si–C component owing to the large scattering efficiency of the C–C bond, which is approximately 40 times higher than that of the Si–C bond [28]). The existence of these three bands implies that clusters corresponding to these three bands coexist in the films, as has generally been previously observed [14,15,26].

A close look at the spectra shows that three types of distinct changes occurred when the absolute value of the bias voltage increased to approximately –80 V: the change of the SiC-related band to a bimodal shape due to the appearance of a new band at approximately 940 cm^{-1}, abrupt wavenumber shifts of the amorphous Si- and C-related scattering bands (from the positions indicated by the dotted line arrows to those indicated by the solid line arrows) and a peak broadening of the amorphous C-related band. The most apparent of the three changes is the enhancement of the SiC band intensity at approximately 940 cm^{-1}, which was observed for all films deposited above the critical bias voltage and deposition temperature. The SiC bands of the films deposited at substrate biases of –80 V and −100 V appear to be composed of bimodal bands (with transverse optic (TO) and longitudinal optic (LO) modes of approximately 780 cm^{-1} and 940 cm^{-1}, respectively.) This is related to the crystallization of the SiC phase since the appearance of the LO phonon band near 940 cm^{-1} corresponds to the microcrystalline modification of the SiC phase [15,29]. This phenomenon can be considered as a type of phase transformation that is induced by the bombardment with gaseous ions (which can be referred to as an ion bombardment induced phase transformation or crystallization): the amorphous SiC phase partially transforms into the nanocrystalline SiC phase, and the remainder is in a state different from that of the parent amorphous SiC phase. A comparison of the microstructural characteristics shown in Fig. 1 with the appearance of the enhanced band at approximately 940 cm^{-1} in the Raman spectra of Fig. 2, represents the close correlation of the shape of the Raman spectra with the formation of the microstructure of the SiC film shown in Fig. 1b. The enhancement of the Raman band intensity at approximately 940 cm^{-1} is very sensitive to the crystallization of the SiC phase and could thus be used to quantify the degree of crystallization of the SiC thin films.

The fact that the wavenumber shifts of both the carbon and Si scattering bands as well as the broadening of the carbon bands occurred at the same time as the bimodal shape change of the SiC scattering band implies that the nature of the short-range ordering inside both the Si and C clusters also changed with the crystallization of the SiC phase, although they remain in an amorphous state. The wavenumber shifts observed in the SiC films have been suggested to be caused by several reasons, including changes in the stoichiometric ratio of the film, the degree of short-range ordering, the size of the clusters, and the defect density [29,30]. Since the concentration ratio was measured by AES to be constant at nearly 1, irrespective of the deposition condition, the possibility of a stoichiometry change effect can be eliminated. The present wavenumber shifts are thus believed to be mainly caused

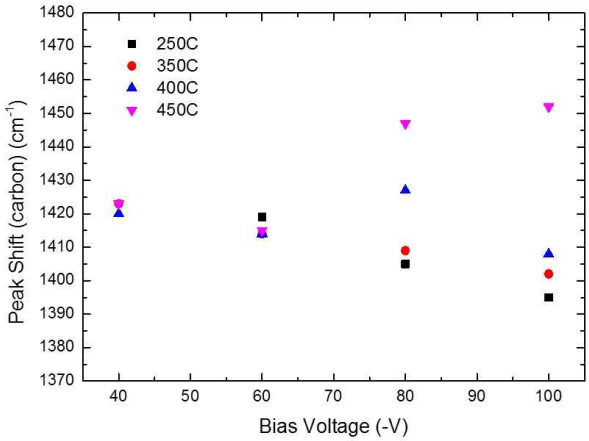

Fig. 3 Variation of the peak shift of the carbon band in the Raman spectra as a function of the substrate bias voltage for SiC films deposited at various temperatures.

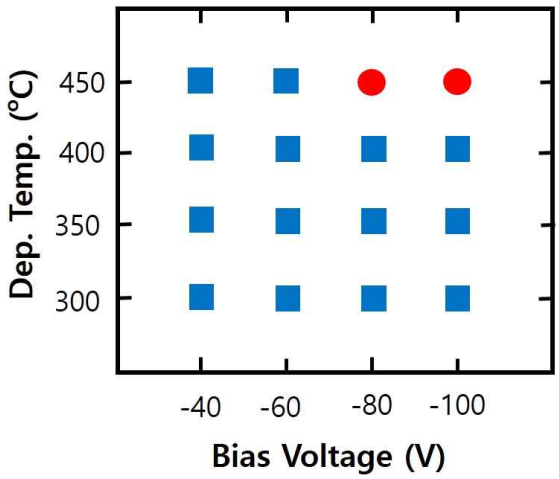

Fig. 4 Phase map of SiC thin film according to substrate bias voltage and deposition temperature (■: amorphous SiC, ●: nanocomposite SiC).

by differences in the short-range ordering in the films or in the size of the clusters.

We plotted the variation of the wavenumber of the carbon band with the bias voltage to clarify their tendency. Fig. 3 shows the variation of the wavenumber of the C–C related scattering band with the substrate bias voltage at various deposition temperatures. The wavenumber monotonically changed to lower values with the increasing bias voltage, in the case of the films deposited at 250 and 350 °C. This means that in the films deposited at these temperatures, the degree of short-range ordering within the carbon clusters gradually deteriorated, or the size of the clusters diminished with increasing bias voltage. The film deposited at 450 °C, however, shows an abrupt wavenumber

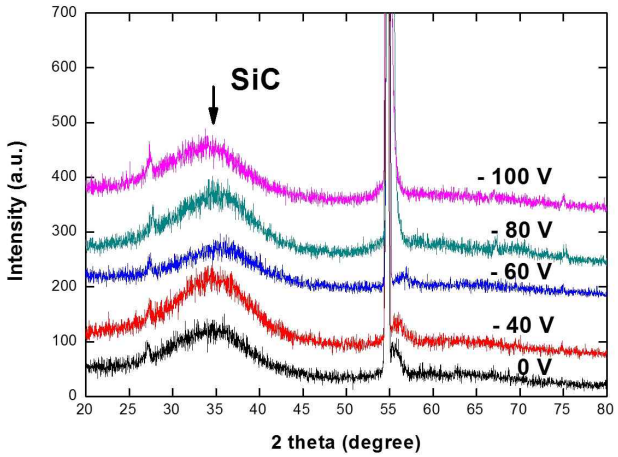

Fig. 5 XRD diffraction patterns of SiC films deposited at 450 °C with various substrate bias voltages.

change to a higher value at a bias voltage above –80 V, which is related to a significant structural change in the carbon clusters under this condition; a similar observation was also made for the silicon-related scattering band, although the magnitude of the variation was small. This condition corresponded to the NCCG formation in the SiC thin film. These results show that the amorphous Si and C clusters also experienced significant structural changes such as the enhancement of the short-range ordering or the increase of the cluster size when the SiC NCCG formed. The above results show that the thermal energy at 250 or 350 °C is not sufficient to restore the atoms displaced by the bombarding ions to their stable positions. At 450 °C, however, the thermal energy (in addition to the kinetic energy of the deposited C atoms delivered by the bombarding ions) may be sufficient for the deposited atoms to have enough time to undergo short-range ordering in the clusters. In addition to the wavenumber change, the carbon-related band was also broadened across the range of critical bias voltages, which is believed to be due to the formation of graphite-like clusters [14]. Such a structure change can broaden the carbon-related scattering band due to the appearance of a G band of carbon at a higher wave number.

On the basis of the results shown in Fig. 1 and 2, the conditions for the formation of the SiC films with the NCCG can be drawn as a map (Fig. 4). Under the deposition conditions of the present sputtering system, a deposition temperature higher than 400 °C was required for the formation of the NCCG in the SiC films, even under the optimum ion bombardment. Thus, it can be concluded that a minimum thermal energy is necessary for the formation of the crystalline SiC phases, even with ion bombardment.

Fig. 5 shows the XRD patterns of the same SiC films as subjected to the Raman spectroscopy measurements shown in Fig. 2. Only one broad band corresponding to the (111) plane of cubic phase SiC was visible. These spectra are typical patterns from an X-ray amorphous phase [22], with no definite diffraction peak originating from a crystalline phase visible. This indicates that the thin films were either in the amorphous phase or consisted of very fine crystalline grains. Different from the Raman spectra shown in Fig. 2, no tangible differences were observed among the films deposited at various substrate bias voltages, irrespective of the formation of the crystalline grains shown in Fig. 1. The XRD analysis is thus not sufficiently sensitive to distinguish the formation of the crystalline phase of the present films.

4. Conclusions

The influences of the substrate bias voltage and deposition temperature on the phase of SiC thin films deposited using an UBM sputtering system were studied. Above a critical bias voltage and deposition temperature, the microstructure of the SiC film appeared to change from an amorphous to a nanocomposite-like structure in which NCCG were embedded in an amorphous SiC matrix. It was proven experimentally that both the bombardment of ions and a minimum thermal energy are mandatory for the formation of the SiC NCCG.

Three different structural analysis methods (TEM, Raman spectroscopy, and XRD) were used to identify the phase of the films. Cross-sectional observations using TEM clearly showed the existence of NCCG in an amorphous SiC matrix. The existence of those grains could also be confirmed via Raman spectroscopic analysis; an enhancement of the scattering band at approximately 940 cm^{-1} was related to the formation of the crystalline phase. The XRD analysis, however, could not definitively demonstrate the existence of the crystalline SiC phases.

Acknowledgments

This work was supported by the KIST Institutional Program (project no. 2E26370). The authors appreciate Mr. Y.H.Choi for his assistance in preparation of the manuscript.

References

1. A. V. Singh, S. Chandra, S. Kumar, and G. Bose, *J. Micromech. Microeng.,* **22**, 025010 (2012).
2. X.-A. Fu, J.L. Dunning, M. Mehregany, and C.A. Zorman, *J. Electrochem. Soc.,* **158**, H675 (2011).
3. J. Trevino, X.-A. Fu, M. Mehregany, and C. A. Zorman, *J. Micromech. Microeng.,* **24**, 065001 (2014).
4. M. Chaker, S. Boily, Y. Diawara, M. El Khakani, E. Gat, A. Jean, H. Lafontaine, and H. Pepin, J. Voyer, J. Kieffer, *J. Vac. Sci. Technol. B*, **10**, 3191 (1992).
5. S.-I. Han, P. Mangat, S. Smith, W. Dauksher, D. Convey, and R. Gregory, *J. Vac. Sci. Technol. A*, **18**, 1225 (2000).
6. M. P. Schmidt, I. Solomon, H. Tran-Quoc, and J. Bullot, *J. Non·Cryst. Solids*, **77**, 849 (1985).
7. A. Mahan, D. Williamson, M. Ruth, and P. Raboisson, *J. Non·Cryst. Solids*, **77**, 861 (1985).
8. Z. Yu, I. Pereyra, and M. Carreno, *Sol. Energy Mater. Sol. Cells*, **66**, 155 (2001).
9. G. Foti, *Appl. Surf. Sci.*, **184**, 20 (2001).
10. P. T. Shaffer, *J. Am. Ceram. Soc.*, **47**, 466 (1964).
11. A. Costa, S. Camargo Jr, C. Achete, and R. Carius, *Thin Solid Films*, **377**, 243 (2000).
12. M. El Khakani, M. Chaker, M. O'Hern, and W. Oliver, *J. Appl. Phys.*, **82**, 4310 (1997).
13. M. El Khakani, M. Chaker, A. Jean, S. Boily, J. Kieffer, M. O'hern, M. Ravet, and F. Rousseaux, *J. Mater. Res.*, **9**, 96 (1994).
14. V. Kulikovsky, P. Boháč, J. Zemek, V. Vorlíček, A. Kurdyumov, and L. Jastrabík, *Diam. Relat. Mater.*, **16**, 167 (2007).
15. V. Kulikovsky, V. Vorlíček, P. Boháč, M. Stranyánek, R. Čtvrtlík, A. Kurdyumov, and L. Jastrabik, *Surf. Coat. Technol.*, **202**, 1738 (2008).
16. F. Liao, S. Girshick, W. Mook, W. Gerberich, and M. Zachariah, *Appl. Phys. Lett.*, **86**, 171913 (2005).
17. K. E. Bae, K. W. Chae, J. K. Park, W. S. Lee, and Y. J. Baik, *Adv. Eng. Mater.*, **18**, 1123 (2016).
18. K.-E. Bae, J.-K. Park, W.-S. Lee, Y.-J. Baik, and K.-W. Chae, *Korean J. Met. Mater.,* **53**, 541 (2015).
19. S. Veprek and A.S. Argon, *J. Vac. Sci. Technol. B*, **20**, 650 (2002).
20. S. Veprek, S. Mukherjee, P. Karvankova, H.-D. Männling, J. He, K. Moto, J. Prochazka, and A. Argon, *J. Vac. Sci. Technol. A*, **21**, 532 (2003).
21. S. Veprek, M.G. Veprek-Heijman, P. Karvankova, and J. Prochazka, *Thin Solid Films*, **476**, 1 (2005).
22. J. Musil, *Physical and mechanical properties of hard nanocomposite films prepared by reactive magnetron sputtering, in: Nanostructured coatings*, p. 407, Springer (2006).
23. J. Musil and M. Jirout, *Surf. Coat. Technol.*, **201**, 5148 (2007).
24. P. Musumeci, R. Reitano, L. Calcagno, F. Roccaforte, A. Makhtari, and M. Grimaldi, *Philos. Mag. B*, **76**, 323 (1997).
25. R. Messier, A. Giri, and R. Roy, *J. Vac. Sci. Technol. A*, **2**, 500 (1984).
26. M. Lattemann, E. Nold, S. Ulrich, H. Leiste, and H. Holleck, *Surf. Coat. Technol.*, **174**, 365 (2003).
27. Y. Inoue, S. Nakashima, A. Mitsuishi, S. Tabata, and S. Tsuboi, *Solid State Commun.*, **48**, 1071 (1983).
28. R. Hillel, M. Maline, F. Gourbilleau, G. Nouet, R. Carles, and A. Mlayah, *Mater. Sci. Eng. A*, **168**, 183 (1993).

29. V. Kulikovsky, V. Vorlíček, P. Boháč, A. Kurdyumov, and L. Jastrabík, *Diam. Relat. Mater.*, **13**, 1350 (2004).
30. A. C. Ferrari and J. Robertson, *Phys. Rev. B*, **61**, 14095 (2000).
31. H. Hobert, H. Dunken, S. Urban, F. Falk, and H. Stafast, *Vib. Spectrosc.*, **29**, 177 (2002).